Does the human placenta express the canonical cell entry mediators for SARS-CoV-2?

Roger Pique-Regi[1,2,3,*], Roberto Romero[1,3-7,*], Adi L. Tarca[2,3,8], Francesca Luca[1,2], Yi Xu[2,3], Adnan Alazizi[1], Yaozhu Leng[2,3], Chaur-Dong Hsu[2,3,9], Nardhy Gomez-Lopez[2,3,10,*]

[1]Center for Molecular Medicine and Genetics, Wayne State University, Detroit, Michigan, USA
[2]Department of Obstetrics and Gynecology, Wayne State University School of Medicine, Detroit, Michigan, USA
[3]Perinatology Research Branch, Division of Obstetrics and Maternal-Fetal Medicine, Division of Intramural Research, *Eunice Kennedy Shriver* National Institute of Child Health and Human Development, National Institutes of Health, U.S. Department of Health and Human Services, Bethesda, Maryland, and Detroit, Michigan, USA
[4]Department of Obstetrics and Gynecology, University of Michigan, Ann Arbor, Michigan, USA
[5]Department of Epidemiology and Biostatistics, Michigan State University, East Lansing, Michigan, USA
[6]Detroit Medical Center, Detroit, Michigan, USA
[7]Department of Obstetrics and Gynecology, Florida International University, Miami, Florida, USA
[8]Department of Computer Science, Wayne State University College of Engineering, Detroit, Michigan, USA
[9]Department of Physiology, Wayne State University School of Medicine, Detroit, Michigan, USA
[10]Department of Department of Biochemistry, Microbiology and Immunology, Wayne State University School of Medicine, Detroit, Michigan, USA

***Corresponding authors:** rpique@wayne.edu; prbchiefstaff@med.wayne.edu; nardhy.gomez-lopez@wayne.edu

Disclosure: The authors report no conflicts of interest.

Funding: This research was supported, in part, by the Perinatology Research Branch, Division of Obstetrics and Maternal-Fetal Medicine, Division of Intramural Research, *Eunice Kennedy Shriver* National Institute of Child Health and Human Development, National Institutes of Health, U.S. Department of Health and Human Services (NICHD/NIH/DHHS); and, in part, with Federal funds from NICHD/NIH/DHHS under Contract No. HHSN275201300006C. N. G-L. is also supported by the Wayne State University Perinatal Initiative in Maternal, Perinatal and Child Health.

R. R. has contributed to this work as part of his official duties as an employee of the United States Federal Government.

ABSTRACT

The pandemic of coronavirus disease 2019 (COVID-19) caused by the severe acute respiratory syndrome coronavirus 2 (SARS-CoV-2) has affected over 3.8 million people, including pregnant women. To date, no consistent evidence of vertical transmission for SARS-CoV-2 exists. This new coronavirus canonically utilizes the angiotensin-converting enzyme 2 (ACE2) receptor and the serine protease TMPRSS2 for cell entry. Herein, building upon our previous single cell study of the placenta (Pique-Regi, 2019), another study, and new single-cell/nuclei RNA-sequencing data, we investigated the expression of ACE2 and TMPRSS2 throughout pregnancy as well as in third-trimester chorioamniotic membranes. We report that co-transcription of ACE2 and TMPRSS2 is negligible, thus not a likely path of vertical transmission for SARS-CoV-2 at any stage of pregnancy. In contrast, receptors for Zika virus and cytomegalovirus which cause congenital infections are highly expressed by placental cell types. These data suggest that SARS-CoV-2 is unlikely to infect the human placenta through the canonical cell entry mediators; yet, other interacting proteins could still play a role in the viral infection.

MAIN TEXT

The placenta serves as the lungs, gut, kidneys, and liver of the fetus [1, 2]. This fetal organ also has major endocrine actions that modulate maternal physiology [1] and, importantly, together with the extraplacental chorioamniotic membranes shield the fetus against microbes from hematogenous dissemination and from invading the amniotic cavity [3]. Indeed, most pathogens that cause hematogenous infections in the mother are not able to reach the fetus, which is largely due to the potent protective mechanisms provided by placental cells (i.e. trophoblast cells: syncytiotrophoblasts and cytotrophoblasts) [4]. Yet, some of these pathogens such as *Toxoplasma gondii*, Rubella virus, herpesvirus (HSV), cytomegalovirus (CMV), and Zika virus (ZIKV), among others, are capable of crossing the placenta and infecting the fetus, causing congenital disease [5, 6].

In December 2019, a local outbreak of pneumonia caused by a novel coronavirus—severe acute respiratory syndrome coronavirus 2 (SARS-CoV-2)—was reported in Wuhan (Hubei, China) [7]. After exposure to SARS-COV-2, susceptible individuals can develop coronavirus disease 2019 (COVID-19) consisting of symptoms that may range from fever and cough to severe respiratory illness; in some cases, COVID-19 is life-threatening [8, 9]. Since the onset of the outbreak, more than 3.8 million COVID-19 cases have been confirmed, accounting for more than 269,000 deaths [10]. This pandemic has now spread throughout the entire world with recent epicenters in Europe (Italy and Spain) and the United States. By April 2019, the states of New York and Michigan were the most affected [10], given that the metropolitan areas of New York City and Detroit possess a large population subject to health disparities such as limited access to health care, chronic exposure to pollution, and pre-existing cardiovascular conditions [11].

Pregnant women and their fetuses represent a high-risk population in light of the COVID-19 outbreak [12-20] since viral infections such as influenza [21-27], varicella [28-32], Ebola [33, 34], and measles [35, 36] show increased severity in this physiological state. Other coronavirus such as SARS-CoV-1 and MERS-CoV have severe effects to both the mother and the fetus, but vertical transmission has not been proven [37-41] albeit these studies included very few number of cases. In contrast with the abovementioned viral infections, only ~15% of pregnant women test positive for SARS-CoV-2 and a small fraction of them are symptomatic [42], most of whom (92%) experience only a mild illness [43]. Thus, the clinical characteristics of pregnant women with COVID-19 appear similar to those of non-pregnant adults [44]. In addition, thus far, no conclusive evidence of vertical transmission has been generated [45-49]. Consistently, infants born to mothers with COVID-19 test negative for SARS-CoV-2, do not develop serious clinical symptoms (e.g., fever, cough, diarrhea, or abnormal radiologic or hematologic evidence), and are promptly discharged from the hospital [50]. Nevertheless, new evidence has emerged suggesting that the fetus can respond to SARS-CoV-2 infection.

Case reports showed that a small fraction of neonates born to women with COVID-19 tested positive for the virus at 1-4 days of life [51, 52]; yet, these neonates subsequently tested negative on day 6-7 [51]. In addition, serological studies revealed that a few neonates born to mothers with COVID-19 had increased concentrations of SARS-CoV-2 immunoglobulin (Ig)M as well as IgG [53, 54]. The elevated concentrations of IgG are likely due to the passive transfer of this immunoglobulin from the mother to the fetus across the placenta. However, the increased levels of IgM suggest that the fetus was infected with SARS-CoV-2 since this immunoglobulin cannot cross the placenta due to its large molecular weight. Nonetheless, all neonates included in the above-mentioned studies tested negative for the virus and did not present any symptoms [53, 54].

More recently, two case reports have been reported where SARS-CoV-2 RNA has been detected in amniotic fluid and placental tissues. In the first case report, the viral RNA was detected in amniotic fluid from a woman who was severely affected and died of COVID-19 [55]. The premature neonate tested negative for SARS-CoV-2 after delivery but 24hr later tested positive [55]. In the second case report, the viral RNA was detected in the placenta and umbilical cord from a woman with severe pre-eclampsia, placental abruption, and other complications; yet, none of the fetal tissues tested positive [56]. Therefore, whether SARS-CoV-2 can reach the fetus by crossing the placenta is still unclear.

Cell entry and spreading of SARS-CoV-2 has been widely thought to depend on the angiotensin-converting enzyme 2 (ACE2) receptor [57, 58] and the serine protease TMPRSS2 [59]. In the study herein, we investigated whether the receptors responsible for SARS-CoV-2 infection are expressed in the human placenta (including the decidual tissues) throughout the three trimesters of pregnancy using publicly available single-cell RNA-sequencing (scRNA-seq) data [60, 61] together with newly generated data (Table S1).

Strikingly, we found that very few cells co-express ACE2 and TMPRSS2 **(Fig. 1A and B)**. Using a very permissive threshold of expression of one transcript per cell, only four cells with co-expression were detected in any of the three trimesters, resulting in an estimated < 1/10,000 cells. Our first-trimester data are in agreement with a prior report showing that there is minimal expression of ACE2 at the human maternal-fetal interface [62]; however, the same dataset was recently used to report the opposite [63]. Nonetheless, the co-expression of ACE2 and TMPRSS2 was not examined by either study. We also evaluated the expression of SARS-CoV2 receptors in the chorioamniotic membranes (also known as the extraplacental membranes) in the third trimester, since these tissues may also serve as a point of entry for microbial invasion of the amniotic cavity and potentially the fetus [64]. Again, co-expression of ACE2 and TMPRSS2 was minimally detected in the chorioamniotic membranes **(Fig. 1A and B)**.

A challenge in scRNA-seq studies is generating high-quality single-cell suspensions containing both rare and difficult-to-dissociate (e.g. multinucleated cells) cell types. This is likely the reason why the reported scRNA-seq studies of the human placenta contain a low fraction of syncytiotrophoblast cells [STB, multinucleated cells forming the outermost fetal component of the placenta in direct contact with the maternal circulation (i.e., intervillous space)] [60, 61, 65]. Therefore, we considered whether the expression of ACE2 and TMPRSS2 was minimally observed in the placental cell types due to the reduced fraction of STB cells (i.e., dissociation bias). To address this possibility, we prepared single-nucleus suspensions of the placental tissues (including the decidua basalis) and performed single-nuclear RNAseq (snRNA-seq), which reduces the dissociation bias against large cells [66]. An important advantage of snRNA-seq is its compatibility with biobank frozen samples; therefore, we pooled 32 placental villi/decidua samples collected in the third trimester (Table S2). This represents the first snRNA-seq study of the placental tissues. A limitation of snRNA-seq is that it has a higher background compared to scRNAseq but this should not affect the analyses reported here. As expected, a larger fraction of STB cells/nuclei was observed using snRNA-seq compared to scRNA-seq **(Fig. 1A)**. Consistent with the scRNAseq analyses, the snRNAseq data demonstrated that co-expression of ACE2 and TMPRSS2 is unlikely in the placental tissues **(Fig. 1B)**. Finally, we explored the co-expression of ACE2 and TMPRSS2 in third-trimester placental tissues by mining two microarray datasets that we have previously reported [67, 68]. These analyses of bulk gene expression data revealed that while ACE2 was detected above background in most of the samples, TMPRSS2 was largely undetected **(Table S3)**. Collectively, these results consistently indicate that the human placental tissues negligibly co-express ACE2 and TMPRSS2. This reduced expression contrasts with the high expression of ACE2 and TMPRSS2 in nasal goblet and ciliated cells within the human

airways, lungs, and gastrointestinal tract, which are targeted during COVID-19 [69-71]. Therefore, our results suggest that vertical transmission of SARS-CoV-2 is unlikely to occur unless facilitated by other concomitant pathological conditions resulting in a breach of the maternal-fetal crosstalk.

There is a possibility, however, that SARS-CoV-2 could infect the human placenta by using alternate entry routes by interacting with other proteins [72]. The expression of additional SARS-CoV-2-related receptors or proteins in the human placenta is shown in **Fig. 2, CoV-Alt**; however, further research is required to test their participation in the pathogenesis of COVID-19. For example, *in vitro* studies suggest that BSG (Basigin, also called CD147 or EMMPRIN, transmembrane glycoprotein belonging to the immunoglobulin superfamily) provides an alternate entry for SARS-CoV-2 when ACE2 and TMPRSS2 are not expressed [73-75]. We found that the placenta and chorioamniotic membranes expressed high levels of BSG throughout pregnancy **(Fig. 2, CoV-Alt)**; yet, this transcript is also widely expressed in all human tissues and cell types **(Fig. S1)**. Therefore, it is unlikely that this protein alone is a sufficient requirement for SARS-CoV-2 viral entry and other proteins may be required to explain the cell-type primarily affected by COVID-19. Moreover, cathepsin L (CSTL) and FURIN may also function as proteases priming the SARS-CoV-2 S protein [76]. We found that these proteases are highly expressed by the placental tissues throughout gestation **(Fig. 2, CoV-Alt).** Nevertheless, these proteases may not provide sufficient levels of priming by themselves [77-79] when tested with SARS-CoV-1, yet this has not been verified for SARS-CoV-2. Given that the placental tissues are enriched in maternal and fetal macrophages [61], and that a subset of these immune cells expressing sialoadhesin (SIGLEC1, also known as CD169) can contribute to viral spread during SARS-CoV-2 infection [80, 81], we also investigated the expression of SIGLEC1 in this study. As expected, SIGLEC1 was expressed by macrophages in the placenta and chorioamniotic membranes and, to a lesser extent, in T cells **(Fig. 2, CoV-Alt)**. However, even if the virus could infect the placental/decidual macrophages expressing SIGLEC1, this is not sufficient for viral spreading. The expression of ADAM17 was also investigated in the placental tissues since this metalloproteinase competes with TMPRSS2 in ACE2 processing [82]. The placenta and chorioamniotic membranes highly expressed ADAM17 **(Fig. S2)**; however, only cleavage by TMPRSS2 results in augmented SARS-S-driven cell entry [82]. While these CoV-Alt molecules may be used for SARS-CoV-2 infection, they are likely to be less efficient than ACE2 and TMPRSS2, which are already targeted for antiviral interventions [59]; yet, new candidate host:viral interacting proteins and possible drugs are being investigated [72].

Given that the main mediators for cell entry of SARS-CoV-2 were minimally expressed by the human placenta, we also investigated whether the receptors for congenital viruses such as CMV and ZIKV, which are known to infect and cross the placenta [5, 6], were detectable using our pipeline. Known receptors for CMV include NRP2 [83], PDFGRA [83], and CD46 [84]. Notably, all of these receptors were highly expressed in several placental cell types **(Fig. 2, CVM and Fig. S2)**. Next, we investigated the expression of the AXL receptor for ZIKV [85, 86] as well as other related molecules such as CD209 [87] and TYRO3 [88]. Consistent with vertical transmission, AXL, the preferred receptor for ZIKV, was highly expressed by the cells of the human placenta and chorioamniotic membranes throughout gestation **(Fig. 2, ZIKV).** The expression of CD206 was mainly found in the maternal and fetal macrophage subsets, as expected [89, 90]. Yet, the expression of TYRO3 was low **(Fig. S2)**, consistent with the view that TAM receptors are not essential for ZIKV infection [91]. The expression of other viral receptors involved in congenital disease was also documented in the placental tissues **(Fig. S2)**.

In conclusion, the single-cell transcriptomic analysis presented herein provides evidence that SARS-CoV-2 is unlikely to infect the placenta and fetus since its canonical receptor and protease, ACE2 and TMPRSS2, are only minimally expressed by the human placenta throughout

pregnancy. In addition, we showed that the SARS-CoV-2 receptors are not expressed by the chorioamniotic membranes in the third trimester. However, viral receptors utilized by CMV, ZIKV, and others are highly expressed by the human placental tissues. While transcript levels do not always correlate with protein expression, our data indicates a low likelihood of placental infection and vertical transmission of SARS-CoV-2. However, it is still possible that the expression of these proteins is much higher in individuals with pregnancy complications related with the renin-angiotensin-aldosterone system, which can alter the expression of ACE2 [92]. The cellular receptors and mechanisms that could be exploited by SARS-CoV-2 are still under investigation [72]; yet, single-cell atlases can help to identify cell types with a similar transcriptional profile to those that are known to participate in COVID-19.

METHODS

Data availability:

Placenta and decidua scRNA-seq data from first-trimester samples were downloaded through ArrayExpress (E-MTAB-6701). Data for third-trimester samples previously collected by our group are available through NIH dbGAP (accession number phs001886.v1.p1), and newly generated second-trimester scRNA-seq and third-trimester snRNA-seq data are being deposited in the same repository (Table S1). All software and R packages used herein are detailed in the "scRNA-seq and snRNA-seq data analysis." Scripts detailing the analyses are also available at https://github.com/piquelab/sclabor.

Sample collection and processing, single-cell/nuclei preparation, library preparation, and sequencing:

Human subjects: Placental tissues were obtained immediately after a clinically indicated delivery from (i) a patient diagnosed with placenta accreta at 18 weeks of gestation and (ii) 32 patients spanning different conditions at the third trimester (Table S2). A sample of the basal plate of the placenta including the decidua basalis and placental villi tissue was (i) dissociated as previously described [61] for scRNA-seq or (ii) preserved in RNAlater and subsequently frozen for snRNA-seq. The collection and use of human materials for research purposes were approved by the Institutional Review Board of the Wayne State University School of Medicine. All participating women provided written informed consent prior to sample collection.

Single-cell preparation: Cells from the placental villi and basal plate were isolated by enzymatic digestion using previously described protocols with modifications [61, 65, 93]. Briefly, placental tissues were homogenized using a gentleMACS Dissociator (Miltenyi Biotec, San Diego, CA) either in an enzyme cocktail from the Umbilical Cord Dissociation Kit (Miltenyi Biotec) or in collagenase A (Sigma Aldrich, St. Louis, MO). After digestion, homogenized tissues were washed with ice-cold 1X phosphate-buffered saline (PBS) and filtered through a cell strainer (Fisher Scientific, Durham, NC). Cell suspensions were then collected and centrifuged at 300 x g for 5 min. at 4ºC. Red blood cells were lysed using a lysing buffer (Life Technologies, Grand Island, NY). Next, the cells were washed with ice-cold 1X PBS and resuspended in 1X PBS for cell counting using an automatic cell counter (Cellometer Auto 2000; Nexcelom Bioscience, Lawrence, MA). Lastly, dead cells were removed from the cell suspensions using the Dead Cell Removal Kit (Miltenyi Biotec), and cells were counted again to determine final viable cell numbers.

Single-cell library preparation using the 10x Genomics platform: Viable cells were utilized for single-cell RNAseq library construction using the Chromium™ Controller and Chromium™ Single Cell 3' Version 3 Kit (10x Genomics, Pleasanton, CA), following the manufacturer's instructions. Briefly, viable cell suspensions were loaded into the Chromium™ Controller to generate gel beads in emulsion (GEM), with each GEM containing a single cell as well as barcoded oligonucleotides. Next, the GEMs were placed in the Veriti 96-well Thermal Cycler (Thermo Fisher Scientific, Wilmington, DE) and reverse transcription was performed in each GEM (GEM-RT). After the reaction, the complementary (c)DNA was cleaned using Silane DynaBeads (Thermo Fisher Scientific) and the SPRIselect Reagent Kit (Beckman Coulter, Indianapolis, IN). Next, the cDNA was amplified using the Veriti 96-well Thermal Cycler and cleaned using the SPRIselect Reagent

Kit. Indexed sequencing libraries were then constructed using the Chromium™ Single Cell 3' Version 3 Kit, following the manufacturer's instructions.
cDNA was fragmented, end-repaired, and A-tailed using the Chromium™ Single Cell 3' Version 3 Kit, following the manufacturer's instructions. Next, adaptor ligation was performed using the Chromium™ Single Cell 3' Version 3 Kit, followed by post-ligation clean-up using the SPRIselect Reagent Kit to obtain the final library constructs, which were then amplified using PCR. After performing a post-sample index double-sided size selection using the SPRIselect Reagent Kit, the quality and quantity of the DNA were analyzed using the Agilent Bioanalyzer High Sensitivity Chip (Agilent Technologies, Wilmington, DE). The Kapa DNA Quantification Kit for Illumina® platforms (Kapa Biosystems, Wilmington, MA) was used to quantify the DNA libraries, following the manufacturer's instructions.

Single-nuclei sample preparation: We developed a new protocol to isolate nuclei from frozen placenta samples, based on DroNc-seq [94] and an early version of the protocol developed by the Martelotto lab [95]. For each placenta sample, 1mm frozen placenta biopsy punches were collected and immediately lysed with ice-cold lysis buffer (10 mM Tris-HCl, pH 7.5, 10 mM NaCl, 3 mM MgCl2, 2% BSA, 0.2 U/µl Protector RNase Inhibitor, and 0.1% IGEPAL-630) for 5 minutes. During incubation the samples were gently mixed by swirling the tube twice and collected by centrifugation at 500 x g for 5 minutes at 4ºC. The process was repeated twice for a total of 3 cycles of lysis (5 minutes long each). Next, the pellets were washed with ice-cold nuclei suspension buffer (1X PBS containing 2% BSA and 0.2 U/µl Protector RNase Inhibitor, ROCHE) and filtered through a 30µm cell strainer (Fisher Scientific). Nuclei suspensions were then collected and centrifuged at 500 x g for 5 minutes at 4ºC. Nuclei were counted using a Countess™ II FL (Thermo Fisher Scientific, Durham, NC). All samples exhibited 100% cell death with DAPI staining, indicative of complete cell lysis. Nuclei were then utilized for single-nuclei RNAseq library construction using the Chromium™ Controller and Chromium™ Single Cell 3' version 2 kit (10x Genomics), following the manufacturer's instructions.

Single-nuclei 10x Genomics library preparation: Briefly, nuclei suspensions for pools of 16 samples were loaded on the Chromium™ Controller to generate GEMs, with each GEM containing a single cell as well as barcoded oligonucleotides. Each pool was loaded on two different channels, for a total of two pools with two replicates each (4 libraries, 32 pregnancy cases). Next, the GEMs were placed in the Veriti 96-well Thermal Cycler, and reverse transcription was performed in each GEM (GEM-RT). After the reaction, the complementary (c)DNA was cleaned using Silane DynaBeads and the SPRIselect Reagent Kit. Next, the cDNA was amplified using the Veriti 96-well Thermal Cycler and cleaned using the SPRIselect Reagent kit. cDNA quality and quantity were analyzed using the Agilent Bioanalyzer High Sensitivity chip.
cDNA was fragmented, end-repaired, and A-tailed using the Chromium™ Single Cell 3' version 2 kit, following the manufacturer's instructions. Next, adapter ligation was performed using the Chromium™ Single Cell 3' version 2 kit followed by post-ligation cleanup using the SPRIselect Reagent kit to obtain the final library constructs, which were then amplified using PCR. After performing a post-sample index double-sided size selection using the SPRIselect Reagent kit, the quality and quantity of the DNA were analyzed using the Agilent Bioanalyzer High Sensitivity chip. The Kapa DNA Quantification Kit for Illumina® platforms was used to quantify the DNA libraries. Phix (Illumina, San Diego, CA), serially diluted at different concentrations, was used as the standard together with a negative and a positive control to quantify and normalize the libraries for loading of the sequencer.

Sequencing: Libraries were sequenced on the Illumina NextSeq 500 in the Luca/Pique-Regi laboratory and in the CMMG Genomics Services Center (GSC). The Illumina 75 Cycle Sequencing Kit was used with 58 cycles for R2, 26 for R1, and 8 for I1.

scRNA-seq and snRNA-seq data analyses:

Raw fastq files were downloaded from previously established resources (as detailed in "Data Availability"), and the new sequencing data were processed using Cell Ranger version 3.0.0 from 10X Genomics for de-multiplexing. The fastq files were then aligned using kallisto [96], and bustools [97] summarized the cell/gene transcript counts in a matrix for each sample, using the "lamanno" workflow for scRNA-seq and the "nucleus" workflow for snRNA-seq. Each sample was then processed using DIEM [98] to eliminate debris and empty droplets for both scRNA-seq and snRNA-seq. To avoid the loss of cells that may express viral receptors, we did not exclude cell doublets from the analyses included in this report, which should have negligible effects on the results and conclusions. All count data matrices were then normalized and combined using the "NormalizeData," "FindVariableFeatures," and "ScaleData" methods implemented in the Seurat package in R (Seurat version 3.1, R version 3.6.1) [99] and [100]. Afterward, the Seurat "RunPCA" function was applied to obtain the first 50 principal components, and the different batches and locations were integrated and harmonized using the Harmony package in R [101]. The top 30 harmony components were then processed using the Seurat "runUMAP" function to embed and visualize the cells in a two-dimensional map via the Uniform Manifold Approximation and Projection for Dimension Reduction (UMAP) algorithm [102, 103]. To label the cells, the Seurat "FindTransferAnchors" and "TransferData" functions were used for each group of locations separately to assign a cell-type identity based on our previously labeled data as reference panel (as performed in [61]). Cell type abbreviations used are: STB, Syncytiotrophoblast; EVT, Extravillous trophoblast; CTB, cytotrophoblast; HSC, hematopoietic stem cell; npiCTB, non proliferative interstitial cytotrophoblast; LED, lymphoid endothelial decidual cell. Visualization of viral receptor gene expression was performed using the ggplot2 [104] package in R with gene expression values scaled to transcripts per million (TPM).

Bulk Gene Expression Data Analysis of ACE2 and TMPRSS2 in the placental tissues:

Gene expression data for the study by Kim et al. [67] was available from the www.ebi.ac.uk/microarray-as/ae/ database (entry ID: E-TABM-577), while data for the study by Toft et al. [68] is available in our data repertoire. The mas5calls function from the *affy* package in Bioconductor was used to determine presence above background of each probeset corresponding to a given gene [105].

Disclosure: The authors report no conflicts of interest.

Funding: This research was supported, in part, by the Perinatology Research Branch, Division of Obstetrics and Maternal-Fetal Medicine, Division of Intramural Research, *Eunice Kennedy Shriver* National Institute of Child Health and Human Development, National Institutes of Health, U.S. Department of Health and Human Services (NICHD/NIH/DHHS); and, in part, with Federal funds from NICHD/NIH/DHHS under Contract No. HHSN275201300006C. N. G-L. and A.L.T. are also supported by the Wayne State University Perinatal Initiative in Maternal, Perinatal and Child Health.

Acknowledgments: We thank the physicians, nurses, and research assistants from the Center for Advanced Obstetrical Care and Research, the Intrapartum Unit, and the PRB Clinical Laboratory for their help with collecting and processing samples.

REFERENCES

1. Burton, G.J. and E. Jauniaux, *What is the placenta?* Am J Obstet Gynecol, 2015. **213**(4 Suppl): p. S6 e1, S6-8.
2. Maltepe, E. and S.J. Fisher, *Placenta: the forgotten organ.* Annu Rev Cell Dev Biol, 2015. **31**: p. 523-52.
3. Ander, S.E., M.S. Diamond, and C.B. Coyne, *Immune responses at the maternal-fetal interface.* Sci Immunol, 2019. **4**(31).
4. Arora, N., et al., *Microbial Vertical Transmission during Human Pregnancy.* Cell Host Microbe, 2017. **21**(5): p. 561-567.
5. Stegmann, B.J. and J.C. Carey, *TORCH Infections. Toxoplasmosis, Other (syphilis, varicella-zoster, parvovirus B19), Rubella, Cytomegalovirus (CMV), and Herpes infections.* Curr Womens Health Rep, 2002. **2**(4): p. 253-8.
6. Coyne, C.B. and H.M. Lazear, *Zika virus - reigniting the TORCH.* Nat Rev Microbiol, 2016. **14**(11): p. 707-715.
7. Dong, E., H. Du, and L. Gardner, *An interactive web-based dashboard to track COVID-19 in real time.* Lancet Infect Dis, 2020.
8. https://www.cdc.gov/coronavirus/2019-ncov/index.html.
9. Wadman M, et al. *How does coronavirus kill? Clinicians trace a ferocious rampage through the body, from brain to toes*. 2020.
10. https://coronavirus.jhu.edu/map.html.
11. https://www.cdc.gov/minorityhealth/CHDIReport.html.
12. Dashraath, P., et al., *Coronavirus Disease 2019 (COVID-19) Pandemic and Pregnancy.* Am J Obstet Gynecol, 2020.
13. Liu, Y., et al., *Clinical manifestations and outcome of SARS-CoV-2 infection during pregnancy.* J Infect, 2020.
14. Rasmussen, S.A., et al., *Coronavirus Disease 2019 (COVID-19) and pregnancy: what obstetricians need to know.* Am J Obstet Gynecol, 2020.
15. Ashokka, B., et al., *Care of the Pregnant Woman with COVID-19 in Labor and Delivery: Anesthesia, Emergency cesarean delivery, Differential diagnosis in the acutely ill parturient, Care of the newborn, and Protection of the healthcare personnel.* Am J Obstet Gynecol, 2020.
16. Della Gatta, A.N., et al., *COVID19 during pregnancy: a systematic review of reported cases.* Am J Obstet Gynecol, 2020.
17. Weber Lebrun, E.E., et al., *COVID-19 Pandemic: Staged Management of Surgical Services for Gynecology and Obstetrics.* Am J Obstet Gynecol, 2020.
18. Tekbali, A., et al., *Pregnant versus non-pregnant SARS-CoV-2 and COVID-19 Hospital Admissions: The first 4 weeks in New York.* Am J Obstet Gynecol, 2020.
19. Hantoushzadeh, S., et al., *Maternal Death Due to COVID-19 Disease.* American Journal of Obstetrics and Gynecology, 2020.
20. Vintzileos, W.S., et al., *Screening all pregnant women admitted to Labor and Delivery for the virus responsible for COVID-19.* American Journal of Obstetrics and Gynecology, 2020.
21. Neuzil, K.M., et al., *Impact of influenza on acute cardiopulmonary hospitalizations in pregnant women.* Am J Epidemiol, 1998. **148**(11): p. 1094-102.
22. Lindsay, L., et al., *Community influenza activity and risk of acute influenza-like illness episodes among healthy unvaccinated pregnant and postpartum women.* Am J Epidemiol, 2006. **163**(9): p. 838-48.
23. Jamieson, D.J., R.N. Theiler, and S.A. Rasmussen, *Emerging infections and pregnancy*. Emerg Infect Dis, 2006. **12**(11): p. 1638-43.

24. Cervantes-Gonzalez, M. and O. Launay, *Pandemic influenza A (H1N1) in pregnant women: impact of early diagnosis and antiviral treatment.* Expert Rev Anti Infect Ther, 2010. **8**(9): p. 981-4.
25. Siston, A.M., et al., *Pandemic 2009 influenza A(H1N1) virus illness among pregnant women in the United States.* JAMA, 2010. **303**(15): p. 1517-25.
26. Mosby, L.G., S.A. Rasmussen, and D.J. Jamieson, *2009 pandemic influenza A (H1N1) in pregnancy: a systematic review of the literature.* Am J Obstet Gynecol, 2011. **205**(1): p. 10-8.
27. Pazos, M., et al., *The influence of pregnancy on systemic immunity.* Immunol Res, 2012. **54**(1-3): p. 254-61.
28. Triebwasser, J.H., et al., *Varicella pneumonia in adults. Report of seven cases and a review of literature.* Medicine (Baltimore), 1967. **46**(5): p. 409-23.
29. Paryani, S.G. and A.M. Arvin, *Intrauterine infection with varicella-zoster virus after maternal varicella.* N Engl J Med, 1986. **314**(24): p. 1542-6.
30. Esmonde, T.F., G. Herdman, and G. Anderson, *Chickenpox pneumonia: an association with pregnancy.* Thorax, 1989. **44**(10): p. 812-5.
31. Haake, D.A., et al., *Early treatment with acyclovir for varicella pneumonia in otherwise healthy adults: retrospective controlled study and review.* Rev Infect Dis, 1990. **12**(5): p. 788-98.
32. Swamy, G.K. and S.K. Dotters-Katz, *Safety and varicella outcomes after varicella zoster immune globulin administration in pregnancy.* Am J Obstet Gynecol, 2019. **221**(6): p. 655-656.
33. Olgun, N.S., *Viral Infections in Pregnancy: A Focus on Ebola Virus.* Curr Pharm Des, 2018. **24**(9): p. 993-998.
34. Muehlenbachs, A., et al., *Ebola Virus Disease in Pregnancy: Clinical, Histopathologic, and Immunohistochemical Findings.* J Infect Dis, 2017. **215**(1): p. 64-69.
35. Christensen, P.E., et al., *Measles in virgin soil, Greenland 1951.* Dan Med Bull, 1954. **1**(1): p. 2-6.
36. Atmar, R.L., J.A. Englund, and H. Hammill, *Complications of measles during pregnancy.* Clin Infect Dis, 1992. **14**(1): p. 217-26.
37. Wong, S.F., K.M. Chow, and M. de Swiet, *Severe Acute Respiratory Syndrome and pregnancy.* BJOG: An International Journal of Obstetrics & Gynaecology, 2003. **110**(7): p. 641-642.
38. Wong, S.F., et al., *Pregnancy and perinatal outcomes of women with severe acute respiratory syndrome.* American Journal of Obstetrics and Gynecology, 2004. **191**(1): p. 292-297.
39. Ng, W.F., et al., *The placentas of patients with severe acute respiratory syndrome: a pathophysiological evaluation.* Pathology, 2006. **38**(3): p. 210-218.
40. Alserehi, H., et al., *Impact of Middle East Respiratory Syndrome coronavirus (MERS-CoV) on pregnancy and perinatal outcome.* BMC Infectious Diseases, 2016. **16**(1): p. 105.
41. Jeong, S.Y., et al., *MERS-CoV Infection in a Pregnant Woman in Korea.* J Korean Med Sci, 2017. **32**(10): p. 1717-1720.
42. Sutton, D., et al., *Universal Screening for SARS-CoV-2 in Women Admitted for Delivery.* N Engl J Med, 2020.
43. Chen, L., et al., *Clinical Characteristics of Pregnant Women with Covid-19 in Wuhan, China.* N Engl J Med, 2020.
44. Yu, N., et al., *Clinical features and obstetric and neonatal outcomes of pregnant patients with COVID-19 in Wuhan, China: a retrospective, single-centre, descriptive study.* Lancet Infect Dis, 2020.

45. Chen, H., et al., *Clinical characteristics and intrauterine vertical transmission potential of COVID-19 infection in nine pregnant women: a retrospective review of medical records.* Lancet, 2020. **395**(10226): p. 809-815.
46. Stower, H., *Lack of maternal-fetal SARS-CoV-2 transmission.* Nat Med, 2020. **26**(3): p. 312.
47. Li, Y., et al., *Lack of Vertical Transmission of Severe Acute Respiratory Syndrome Coronavirus 2, China.* Emerg Infect Dis, 2020. **26**(6).
48. Yan, J., et al., *Coronavirus disease 2019 (COVID-19) in pregnant women: A report based on 116 cases.* American Journal of Obstetrics and Gynecology, 2020.
49. Lamouroux, A., et al., *Evidence for and against vertical transmission for SARS-CoV-2 (COVID-19)* American Journal of Obstetrics and Gynecology, 2020.
50. Chen, Y., et al., *Infants Born to Mothers With a New Coronavirus (COVID-19).* Front Pediatr, 2020. **8**: p. 104.
51. Zeng, L., et al., *Neonatal Early-Onset Infection With SARS-CoV-2 in 33 Neonates Born to Mothers With COVID-19 in Wuhan, China.* JAMA Pediatr, 2020.
52. Alzamora, M.C., et al., *Severe COVID-19 during Pregnancy and Possible Vertical Transmission.* Am J Perinatol, 2020.
53. Zeng, H., et al., *Antibodies in Infants Born to Mothers With COVID-19 Pneumonia.* JAMA, 2020.
54. Dong, L., et al., *Possible Vertical Transmission of SARS-CoV-2 From an Infected Mother to Her Newborn.* JAMA, 2020.
55. Zamaniyan, M., et al., *Preterm delivery in pregnant woman with critical COVID-19 pneumonia and vertical transmission.* Prenat Diagn, 2020.
56. Hosier, H., et al., *SARS-CoV-2 Infection of the Placenta.* medRxiv, 2020: p. 2020.04.30.20083907.
57. Shang, J., et al., *Structural basis of receptor recognition by SARS-CoV-2.* Nature, 2020.
58. Wang, Q., et al., *Structural and Functional Basis of SARS-CoV-2 Entry by Using Human ACE2.* Cell, 2020.
59. Hoffmann, M., et al., *SARS-CoV-2 Cell Entry Depends on ACE2 and TMPRSS2 and Is Blocked by a Clinically Proven Protease Inhibitor.* Cell, 2020. **181**(2): p. 271-280 e8.
60. Vento-Tormo, R., et al., *Single-cell reconstruction of the early maternal-fetal interface in humans.* Nature, 2018. **563**(7731): p. 347-353.
61. Pique-Regi, R., et al., *Single cell transcriptional signatures of the human placenta in term and preterm parturition.* Elife, 2019. **8**.
62. Zheng, Q.-L., T. Duan, and L.-P. Jin, *Single-cell RNA expression profiling of ACE2 and AXL in the human maternal–Fetal interface.* Reproductive and Developmental Medicine, 2020. **4**(1): p. 7-10.
63. Li, M., et al., *The SARS-CoV-2 receptor ACE2 expression of maternal-fetal interface and fetal organs by single-cell transcriptome study.* PLoS One, 2020. **15**(4): p. e0230295.
64. Kim, C.J., et al., *Acute chorioamnionitis and funisitis: definition, pathologic features, and clinical significance.* Am J Obstet Gynecol, 2015. **213**(4 Suppl): p. S29-52.
65. Tsang, J.C.H., et al., *Integrative single-cell and cell-free plasma RNA transcriptomics elucidates placental cellular dynamics.* Proc Natl Acad Sci U S A, 2017. **114**(37): p. E7786-E7795.
66. Wu, H., et al., *Advantages of Single-Nucleus over Single-Cell RNA Sequencing of Adult Kidney: Rare Cell Types and Novel Cell States Revealed in Fibrosis.* J Am Soc Nephrol, 2019. **30**(1): p. 23-32.
67. Kim, M.J., et al., *Villitis of unknown etiology is associated with a distinct pattern of chemokine up-regulation in the feto-maternal and placental compartments: implications for conjoint maternal allograft rejection and maternal anti-fetal graft-versus-host disease.* J Immunol, 2009. **182**(6): p. 3919-27.

68. Toft, J.H., et al., *Whole-genome microarray and targeted analysis of angiogenesis-regulating gene expression (ENG, FLT1, VEGF, PIGF) in placentas from pre-eclamptic and small-for-gestational-age pregnancies.* J Matern Fetal Neonatal Med, 2008. **21**(4): p. 267-73.
69. Sungnak, W., et al., *SARS-CoV-2 entry factors are highly expressed in nasal epithelial cells together with innate immune genes.* Nature Medicine, 2020.
70. Muus, C., et al., *Integrated analyses of single-cell atlases reveal age, gender, and smoking status associations with cell type-specific expression of mediators of SARS-CoV-2 viral entry and highlights inflammatory programs in putative target cells.* bioRxiv, 2020: p. 2020.04.19.049254.
71. Wang, A., et al., *Single Nucleus Multiomic Profiling Reveals Age-Dynamic Regulation of Host Genes Associated with SARS-CoV-2 Infection.* bioRxiv, 2020: p. 2020.04.12.037580.
72. Gordon, D.E., et al., *A SARS-CoV-2 protein interaction map reveals targets for drug repurposing.* Nature, 2020.
73. Blanco-Melo, D., et al., *SARS-CoV-2 launches a unique transcriptional signature from in vitro, ex vivo, and in vivo systems.* bioRxiv, 2020: p. 2020.03.24.004655.
74. Wang, K., et al., *SARS-CoV-2 invades host cells via a novel route: CD147-spike protein.* bioRxiv, 2020: p. 2020.03.14.988345.
75. Ulrich, H. and M.M. Pillat, *CD147 as a Target for COVID-19 Treatment: Suggested Effects of Azithromycin and Stem Cell Engagement.* Stem Cell Rev Rep, 2020.
76. Lukassen, S., et al., *SARS-CoV-2 receptor ACE2 and TMPRSS2 are primarily expressed in bronchial transient secretory cells.* EMBO J, 2020: p. e105114.
77. Shirato, K., et al., *Clinical Isolates of Human Coronavirus 229E Bypass the Endosome for Cell Entry.* J Virol, 2017. **91**(1).
78. Shirato, K., M. Kawase, and S. Matsuyama, *Wild-type human coronaviruses prefer cell-surface TMPRSS2 to endosomal cathepsins for cell entry.* Virology, 2018. **517**: p. 9-15.
79. Iwata-Yoshikawa, N., et al., *TMPRSS2 Contributes to Virus Spread and Immunopathology in the Airways of Murine Models after Coronavirus Infection.* J Virol, 2019. **93**(6).
80. chen, y., et al., *The Novel Severe Acute Respiratory Syndrome Coronavirus 2 (SARS-CoV-2) Directly Decimates Human Spleens and Lymph Nodes.* medRxiv, 2020: p. 2020.03.27.20045427.
81. Park, M.D., *Macrophages: a Trojan horse in COVID-19?* Nat Rev Immunol, 2020.
82. Heurich, A., et al., *TMPRSS2 and ADAM17 cleave ACE2 differentially and only proteolysis by TMPRSS2 augments entry driven by the severe acute respiratory syndrome coronavirus spike protein.* J Virol, 2014. **88**(2): p. 1293-307.
83. Martinez-Martin, N., et al., *An Unbiased Screen for Human Cytomegalovirus Identifies Neuropilin-2 as a Central Viral Receptor.* Cell, 2018. **174**(5): p. 1158-1171 e19.
84. Stein, K.R., et al., *CD46 facilitates entry and dissemination of human cytomegalovirus.* Nat Commun, 2019. **10**(1): p. 2699.
85. Richard, A.S., et al., *AXL-dependent infection of human fetal endothelial cells distinguishes Zika virus from other pathogenic flaviviruses.* Proc Natl Acad Sci U S A, 2017. **114**(8): p. 2024-2029.
86. Persaud, M., et al., *Infection by Zika viruses requires the transmembrane protein AXL, endocytosis and low pH.* Virology, 2018. **518**: p. 301-312.
87. Carbaugh, D.L., R.S. Baric, and H.M. Lazear, *Envelope Protein Glycosylation Mediates Zika Virus Pathogenesis.* J Virol, 2019. **93**(12).
88. Oliveira, L.G. and J.P.S. Peron, *Viral receptors for flaviviruses: Not only gatekeepers.* J Leukoc Biol, 2019. **106**(3): p. 695-701.

89. Svensson, J., et al., *Macrophages at the fetal-maternal interface express markers of alternative activation and are induced by M-CSF and IL-10.* J Immunol, 2011. **187**(7): p. 3671-82.
90. Swieboda, D., et al., *Baby's First Macrophage: Temporal Regulation of Hofbauer Cell Phenotype Influences Ligand-Mediated Innate Immune Responses across Gestation.* The Journal of Immunology, 2020: p. ji1901185.
91. Hastings, A.K., et al., *TAM Receptors Are Not Required for Zika Virus Infection in Mice.* Cell Rep, 2017. **19**(3): p. 558-568.
92. Alexandre, J., et al., *Renin-angiotensin-aldosterone system and COVID-19 infection.* Ann Endocrinol (Paris), 2020.
93. Xu, Y., et al., *Isolation of Leukocytes from the Human Maternal-fetal Interface.* J Vis Exp, 2015(99): p. e52863.
94. Habib, N., et al., *Massively parallel single-nucleus RNA-seq with DroNc-seq.* Nat Methods, 2017. **14**(10): p. 955-958.
95. dx.doi.org/10.17504/protocols.io.3eqgjdw.
96. Bray, N.L., et al., *Near-optimal probabilistic RNA-seq quantification.* Nat Biotechnol, 2016. **34**(5): p. 525-7.
97. Melsted, P., et al., *Modular and efficient pre-processing of single-cell RNA-seq.* bioRxiv, 2019: p. 673285.
98. Alvarez, M., et al., *Enhancing droplet-based single-nucleus RNA-seq resolution using the semi-supervised machine learning classifier DIEM.* bioRxiv, 2019: p. 786285.
99. Hafemeister, C. and R. Satija, *Normalization and variance stabilization of single-cell RNA-seq data using regularized negative binomial regression.* Genome Biology, 2019. **20**(1): p. 296.
100. Stuart, T., et al., *Comprehensive Integration of Single-Cell Data.* Cell, 2019. **177**(7): p. 1888-1902 e21.
101. Korsunsky, I., et al., *Fast, sensitive and accurate integration of single-cell data with Harmony.* Nature Methods, 2019. **16**(12): p. 1289-1296.
102. https://arxiv.org/abs/1802.03426.
103. Becht, E., et al., *Dimensionality reduction for visualizing single-cell data using UMAP.* Nat Biotechnol, 2018.
104. Wickham, H., *ggplot2.* WIREs Computational Statistics, 2011. **3**(2): p. 180-185.
105. Gautier, L., et al., *affy—analysis of Affymetrix GeneChip data at the probe level.* Bioinformatics, 2004. **20**(3): p. 307-315.

Figure Captions

Figure 1. Transcriptional map of the human placenta, including the decidua, in the three trimesters of pregnancy. A. Uniform Manifold Approximation Plot (UMAP), where dots represent single cells/nuclei and are colored by cell type (abbreviations used are: STB, Syncytiotrophoblast; EVT, Extravillous trophoblast; CTB, cytotrophoblast; HSC, hematopoietic stem cell; npiCTB, non proliferative interstitial cytotrophoblast; LED, lymphoid endothelial decidual cell) **B**. UMAP plot with cells/nuclei co-expressing one or more transcripts for ACE2 and TMPRSS2, genes that are necessary for SARS-CoV-2 viral infection and spreading, in red.

Figure 2. Dot plot depicting the expression of different viral receptors/molecules used by SARS-CoV-2, ZIKV, and CMV. Each row represents a different cell type, and columns are grouped first by virus type, receptor/molecule gene, and placental tissue/time-of sampling (1DP, 2DP and 3DP represent the first, second, and third trimester, 3Nuc represents the third trimester nuclei, and 3CAM represents the third trimester chorioamniotic membranes). The size of the dot represents the proportion of cells that express the receptor with more than zero transcripts, and the color represents the average gene expression for the subset of cells expressing that gene in transcripts per million (TPM). Cell type abbreviations used are: STB, Syncytiotrophoblast; EVT, Extravillous trophoblast; CTB, cytotrophoblast; HSC, hematopoietic stem cell; npiCTB, non proliferative interstitial cytotrophoblast; LED, lymphoid endothelial decidual cell.

Figure S1. Gene expression values for BSG across tissues collected by the GTEx project. For each tissue, a violin plot and a boxplot describe the variation in gene expression levels for BSG across all of the samples collected by the project sorted left to right by median gene expression (plot generated through the GTEx portal).

Figure S2. Dot plot depicting the expression of different viral receptors/molecules used by virus that caused congenital infection. Each row represents a different cell type, and columns are grouped first by virus type, receptor/molecule gene, and placental tissue/time-of sampling (1DP, 2DP and 3DP represent the first, second and third trimester, 3Nuc represents the third trimester nuclei, and 3CAM represents the third trimester chorioamniotic membranes). The size of the dot represents the proportion of cells that express the receptor with more than zero transcripts, and the color represents the average gene expression for the subset of cells expressing that gene in transcripts per million (TPM). Cell type abbreviations used are: STB, Syncytiotrophoblast; EVT, Extravillous trophoblast; CTB, cytotrophoblast; HSC, hematopoietic stem cell; npiCTB, non proliferative interstitial cytotrophoblast; LED, lymphoid endothelial decidual cell.

Table S1. Summary of all the single cell resources analyzed using existing and new data.

Table S2. Clinical and demographic characteristics of the study population from which placental samples were collected for snRNAseq studies.

Table S3. Bulk Gene Expression Data Analysis of ACE2 and TMPRSS2 in the placental tissues.

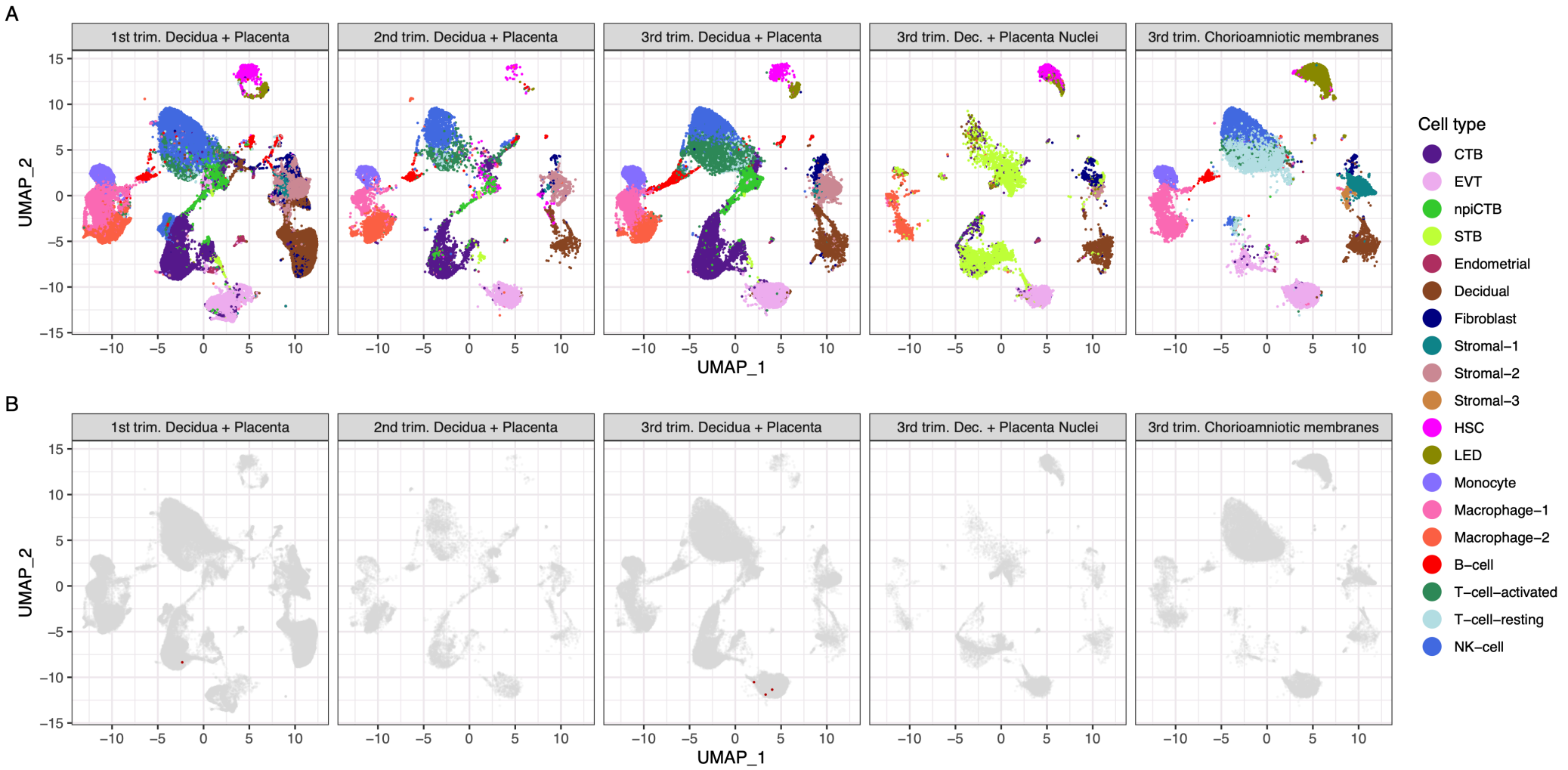
A
B
1st trim. Decidua + Placenta
2nd trim. Decidua + Placenta
3rd trim. Decidua + Placenta
3rd trim. Dec. + Placenta Nuclei
3rd trim. Chorioamniotic membranes
UMAP_1
UMAP_2
Cell type
CTB
EVT
npiCTB
STB
Endometrial
Decidual
Fibroblast
Stromal–1
Stromal–2
Stromal–3
HSC
LED
Monocyte
Macrophage–1
Macrophage–2
B–cell
T–cell–activated
T–cell–resting
NK–cell

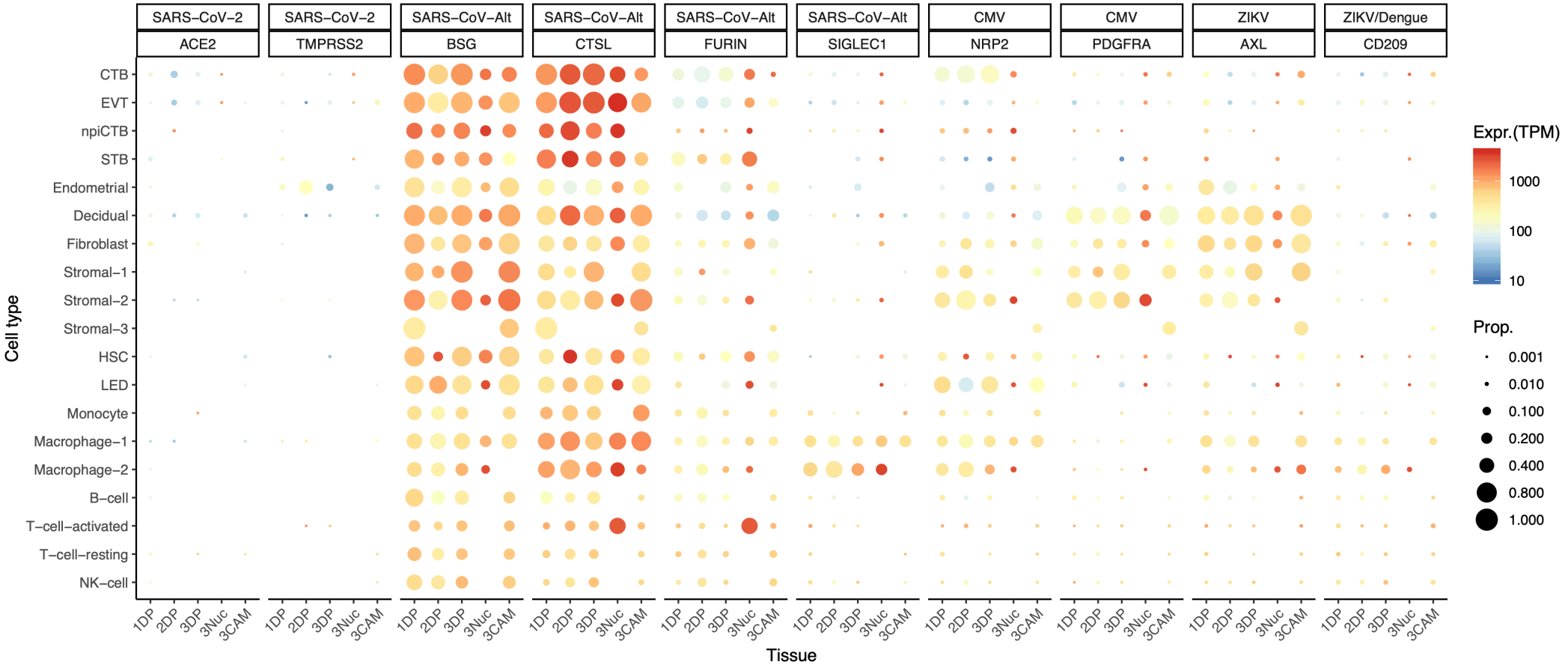
SARS–CoV–2
ACE2
SARS–CoV–2
TMPRSS2
SARS–CoV–Alt
BSG
SARS–CoV–Alt
CTSL
SARS–CoV–Alt
FURIN
SARS–CoV–Alt
SIGLEC1
CMV
NRP2
CMV
PDGFRA
ZIKV
AXL
ZIKV/Dengue
CD209
CTB
EVT
npiCTB
STB
Endometrial
Decidual
Fibroblast
Stromal–1
Stromal–2
Stromal–3
HSC
LED
Monocyte
Macrophage–1
Macrophage–2
B–cell
T–cell–activated
T–cell–resting
NK–cell
Cell type
1DP
2DP
3DP
3Nuc
3CAM
Tissue
Expr.(TPM)
1000
100
10
Prop.
0.001
0.010
0.100
0.200
0.400
0.800
1.000

Supplementary Material

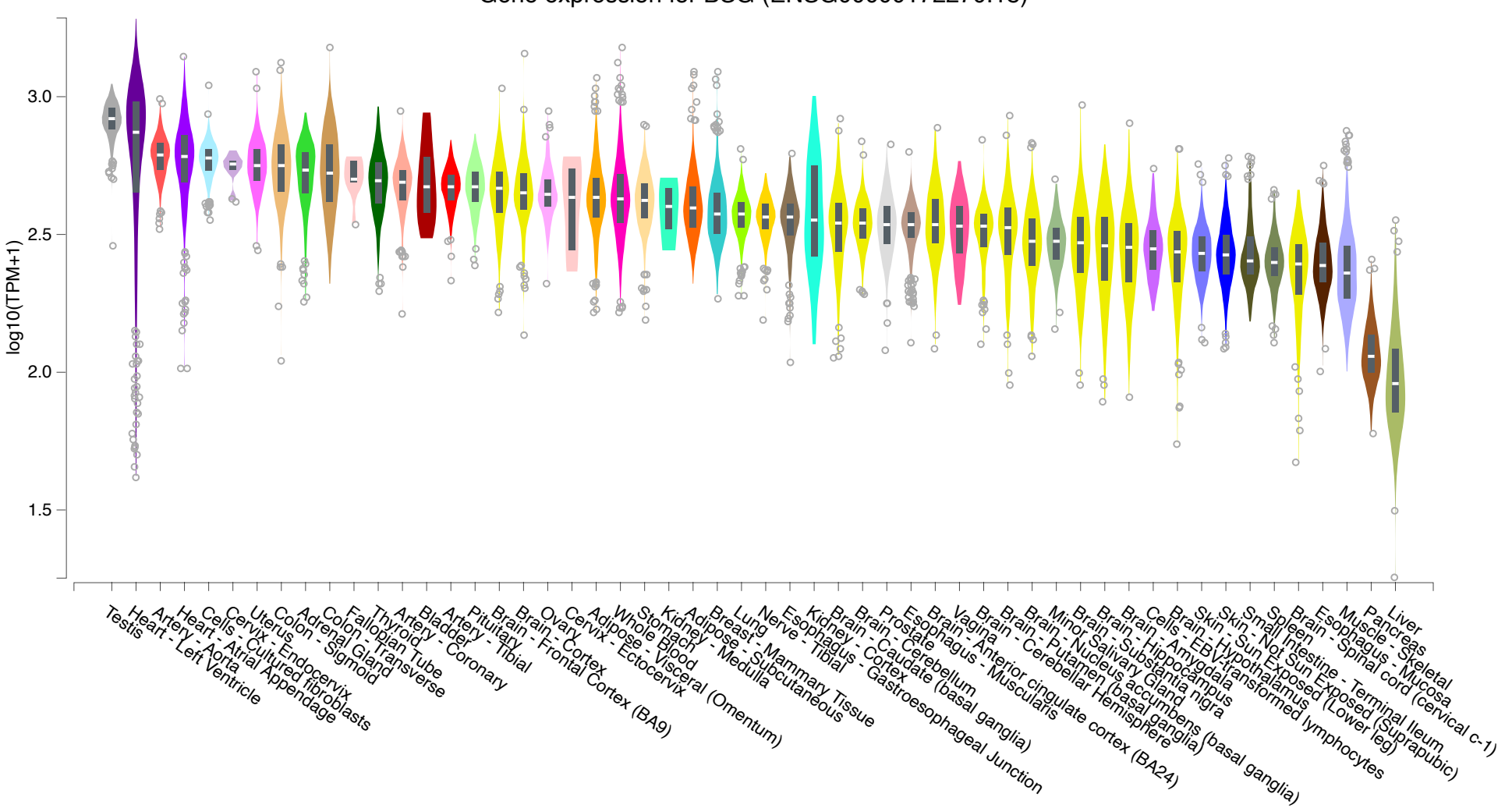
Gene expression for BSG (ENSG00000172270.18)
log10(TPM+1)
3.0
2.5
2.0
1.5
Testis
Heart - Left Ventricle
Artery - Aorta
Heart - Atrial Appendage
Cells - Cultured fibroblasts
Cervix - Endocervix
Uterus
Colon - Sigmoid
Adrenal Gland
Colon - Transverse
Fallopian Tube
Thyroid
Artery - Coronary
Bladder
Artery - Tibial
Pituitary
Brain - Frontal Cortex (BA9)
Brain - Cortex
Ovary
Cervix - Ectocervix
Adipose - Visceral (Omentum)
Whole Blood
Stomach
Kidney - Medulla
Adipose - Subcutaneous
Breast - Mammary Tissue
Lung
Nerve - Tibial
Esophagus - Gastroesophageal Junction
Kidney - Cortex
Brain - Caudate (basal ganglia)
Brain - Cerebellum
Prostate
Esophagus - Muscularis
Brain - Anterior cingulate cortex (BA24)
Vagina
Brain - Cerebellar Hemisphere
Brain - Putamen (basal ganglia)
Brain - Nucleus accumbens (basal ganglia)
Minor Salivary Gland
Brain - Substantia nigra
Brain - Hippocampus
Brain - Amygdala
Cells - EBV-transformed lymphocytes
Skin - Sun Exposed (Lower leg)
Skin - Not Sun Exposed (Suprapubic)
Hypothalamus
Small Intestine - Terminal Ileum
Spleen
Esophagus - Spinal cord (cervical c-1)
Brain - Mucosa
Muscle - Skeletal
Pancreas
Liver

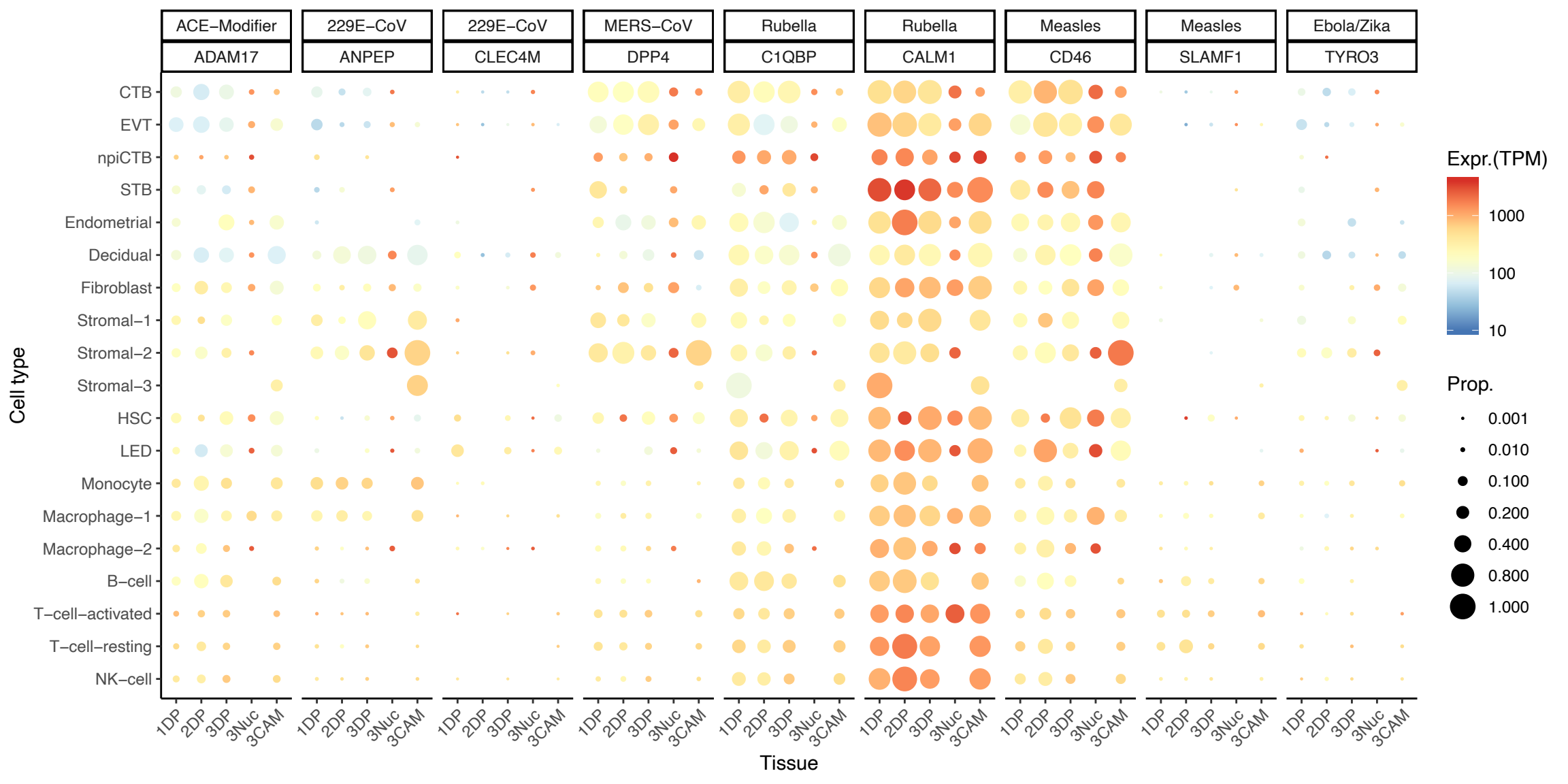
ACE−Modifier
ADAM17
229E−CoV
ANPEP
229E−CoV
CLEC4M
MERS−CoV
DPP4
Rubella
C1QBP
Rubella
CALM1
Measles
CD46
Measles
SLAMF1
Ebola/Zika
TYRO3
Cell type
CTB
EVT
npiCTB
STB
Endometrial
Decidual
Fibroblast
Stromal−1
Stromal−2
Stromal−3
HSC
LED
Monocyte
Macrophage−1
Macrophage−2
B−cell
T−cell−activated
T−cell−resting
NK−cell
1DP
2DP
3DP
3Nuc
3CAM
Tissue
Expr.(TPM)
1000
100
10
Prop.
0.001
0.010
0.100
0.200
0.400
0.800
1.000

Table S1: Summary of all the single cell resources analyzed using existing and new data.

Library ID	Type	Study	Location	Location description	#Pooled	#Cells	Avg. #UMI	Avg. #Genes
HPL20289_R_PVBP_1	scRNA-seq 10X 3' v3	New, this study	2DP	2nd trim. Decidua + Placenta	1	6340	9900	2057
HPL20289_R_PVBP_2	scRNA-seq 10X 3' v3	New, this study	2DP	2nd trim. Decidua + Placenta	1	6850	9810	1910
CC7-1	snRNA-seq 10X 3' v2	New, this study	3Nuc	3rd trim. Dec. + Placenta Nuclei	16	2454	1111	473
CC7-2	snRNA-seq 10X 3' v2	New, this study	3Nuc	3rd trim. Dec. + Placenta Nuclei	16	2759	1199	519
CC8-1	snRNA-seq 10X 3' v2	New, this study	3Nuc	3rd trim. Dec. + Placenta Nuclei	16	3831	1102	530
CC8-2	snRNA-seq 10X 3' v2	New, this study	3Nuc	3rd trim. Dec. + Placenta Nuclei	16	4267	1098	518
s1DB	scRNA-seq 10X 3' v2	Pique-Regi et al. (2019)	3DP	3rd trim. Decidua + Placenta	1	2537	6560	1381
s2DB	scRNA-seq 10X 3' v2	Pique-Regi et al. (2019)	3DP	3rd trim. Decidua + Placenta	1	2285	3695	967
s2P	scRNA-seq 10X 3' v2	Pique-Regi et al. (2019)	3DP	3rd trim. Decidua + Placenta	1	2448	5475	1431
s3DB	scRNA-seq 10X 3' v2	Pique-Regi et al. (2019)	3DP	3rd trim. Decidua + Placenta	1	2321	4477	1061
s3P	scRNA-seq 10X 3' v2	Pique-Regi et al. (2019)	3DP	3rd trim. Decidua + Placenta	1	2412	9160	2047
s4DB	scRNA-seq 10X 3' v2	Pique-Regi et al. (2019)	3DP	3rd trim. Decidua + Placenta	1	3064	6124	1539
s4P	scRNA-seq 10X 3' v2	Pique-Regi et al. (2019)	3DP	3rd trim. Decidua + Placenta	1	2877	8196	2003
s5DB	scRNA-seq 10X 3' v2	Pique-Regi et al. (2019)	3DP	3rd trim. Decidua + Placenta	1	4486	3644	950
s5P	scRNA-seq 10X 3' v2	Pique-Regi et al. (2019)	3DP	3rd trim. Decidua + Placenta	1	2961	4847	1280
s6DB	scRNA-seq 10X 3' v2	Pique-Regi et al. (2019)	3DP	3rd trim. Decidua + Placenta	1	3618	7034	1600
s6P	scRNA-seq 10X 3' v2	Pique-Regi et al. (2019)	3DP	3rd trim. Decidua + Placenta	1	1228	10924	2359
s7DB	scRNA-seq 10X 3' v2	Pique-Regi et al. (2019)	3DP	3rd trim. Decidua + Placenta	1	2737	8983	1811
s7P	scRNA-seq 10X 3' v2	Pique-Regi et al. (2019)	3DP	3rd trim. Decidua + Placenta	1	2479	11049	2159
s8DB	scRNA-seq 10X 3' v2	Pique-Regi et al. (2019)	3DP	3rd trim. Decidua + Placenta	1	2986	6265	1404
s8P	scRNA-seq 10X 3' v2	Pique-Regi et al. (2019)	3DP	3rd trim. Decidua + Placenta	1	3344	12233	2588
s9DB	scRNA-seq 10X 3' v2	Pique-Regi et al. (2019)	3DP	3rd trim. Decidua + Placenta	1	3916	5615	1243
s1W	scRNA-seq 10X 3' v2	Pique-Regi et al. (2019)	3CAM	3rd trim. Chorioamniotic membranes	1	2921	5342	1467
s2W	scRNA-seq 10X 3' v2	Pique-Regi et al. (2019)	3CAM	3rd trim. Chorioamniotic membranes	1	2836	6397	1750
s3W	scRNA-seq 10X 3' v2	Pique-Regi et al. (2019)	3CAM	3rd trim. Chorioamniotic membranes	1	1961	9591	1914
s4W	scRNA-seq 10X 3' v2	Pique-Regi et al. (2019)	3CAM	3rd trim. Chorioamniotic membranes	1	2586	6672	1645
s5W	scRNA-seq 10X 3' v2	Pique-Regi et al. (2019)	3CAM	3rd trim. Chorioamniotic membranes	1	1966	4668	1266
s6W	scRNA-seq 10X 3' v2	Pique-Regi et al. (2019)	3CAM	3rd trim. Chorioamniotic membranes	1	4813	1682	592
s7W	scRNA-seq 10X 3' v2	Pique-Regi et al. (2019)	3CAM	3rd trim. Chorioamniotic membranes	1	3207	4507	1175
s8W	scRNA-seq 10X 3' v2	Pique-Regi et al. (2019)	3CAM	3rd trim. Chorioamniotic membranes	1	5037	7069	1708
s9W	scRNA-seq 10X 3' v2	Pique-Regi et al. (2019)	3CAM	3rd trim. Chorioamniotic membranes	1	3938	7483	1589
FCA7167219	scRNA-seq 10X 3' v2	Vento-Tormo et al. (2018)	1DP	1st trim. Decidua + Placenta	1	716	3591	836
FCA7167221	scRNA-seq 10X 3' v2	Vento-Tormo et al. (2018)	1DP	1st trim. Decidua + Placenta	1	1252	3607	941
FCA7167222	scRNA-seq 10X 3' v2	Vento-Tormo et al. (2018)	1DP	1st trim. Decidua + Placenta	1	1928	9790	1872
FCA7167223	scRNA-seq 10X 3' v2	Vento-Tormo et al. (2018)	1DP	1st trim. Decidua + Placenta	1	8080	2732	895
FCA7167224	scRNA-seq 10X 3' v2	Vento-Tormo et al. (2018)	1DP	1st trim. Decidua + Placenta	1	2232	6132	1675
FCA7167226	scRNA-seq 10X 3' v2	Vento-Tormo et al. (2018)	1DP	1st trim. Decidua + Placenta	1	5775	7415	1918
FCA7196218	scRNA-seq 10X 3' v2	Vento-Tormo et al. (2018)	1DP	1st trim. Decidua + Placenta	1	9028	2203	828
FCA7196219	scRNA-seq 10X 3' v2	Vento-Tormo et al. (2018)	1DP	1st trim. Decidua + Placenta	1	3704	8209	1971
FCA7196220	scRNA-seq 10X 3' v2	Vento-Tormo et al. (2018)	1DP	1st trim. Decidua + Placenta	1	7338	6139	1862
FCA7196224	scRNA-seq 10X 3' v2	Vento-Tormo et al. (2018)	1DP	1st trim. Decidua + Placenta	1	7930	4028	1182
FCA7196225	scRNA-seq 10X 3' v2	Vento-Tormo et al. (2018)	1DP	1st trim. Decidua + Placenta	1	4121	6144	1511
FCA7196226	scRNA-seq 10X 3' v2	Vento-Tormo et al. (2018)	1DP	1st trim. Decidua + Placenta	1	3380	15098	2564
FCA7474062	scRNA-seq 10X 3' v2	Vento-Tormo et al. (2018)	1DP	1st trim. Decidua + Placenta	1	2149	6351	1523
FCA7474063	scRNA-seq 10X 3' v2	Vento-Tormo et al. (2018)	1DP	1st trim. Decidua + Placenta	1	2715	15947	2703
FCA7474064	scRNA-seq 10X 3' v2	Vento-Tormo et al. (2018)	1DP	1st trim. Decidua + Placenta	1	4941	13354	2889
FCA7474065	scRNA-seq 10X 3' v2	Vento-Tormo et al. (2018)	1DP	1st trim. Decidua + Placenta	1	4878	13479	2855
FCA7474068	scRNA-seq 10X 3' v2	Vento-Tormo et al. (2018)	1DP	1st trim. Decidua + Placenta	1	4298	15640	2534
FCA7511881	scRNA-seq 10X 3' v2	Vento-Tormo et al. (2018)	1DP	1st trim. Decidua + Placenta	1	2072	2214	530
FCA7511882	scRNA-seq 10X 3' v2	Vento-Tormo et al. (2018)	1DP	1st trim. Decidua + Placenta	1	2368	10295	1915
FCA7511884	scRNA-seq 10X 3' v2	Vento-Tormo et al. (2018)	1DP	1st trim. Decidua + Placenta	1	4534	9945	2090

Table S2. Clinical and demographic characteristics of the study population from which placental samples were collected for snRNAseq studies

	Study group (n=32)
Clinical parameters	
Maternal age (years; median [IQR])	25 (21.8-29)
Body mass index (kg/m^2; median [IQR])	27.8 (21.7-31.6)[a]
Primiparity	15.6% (5/32)
Cesarean section	59.4% (19/32)
Gestational age at delivery (weeks; median [IQR])	36.9 (32.9-39.1)
Birthweight (g; median [IQR])	2802.5 (1833.8-3233.8)
Ethnicity	
African-American	81.3% (26/32)
Caucasian	6.2% (2/32)
Other	12.5% (4/32)

Data are given as median (interquartile range, IQR) and percentage (n/N)

[a] One missed data

Table S3. Bulk Gene Expression Data Analysis of ACE2 and TMPRSS2 in the placental tissues

Study	Affymetrix probeset	Symbol	Log_2 Average Expression	% of samples detected above background
Kim et al.	219962_at	ACE2	4.61	90%
Kim et al.	222257_s_at	ACE2	5.71	70%
Kim et al.	205102_at	TMPRSS2	5.97	10%
Kim et al.	1570433_at	TMPRSS2	3.37	0%
Kim et al.	211689_s_at	TMPRSS2	2.96	0%
Kim et al.	226553_at	TMPRSS2	6.02	0%
Toft et al.	219962_at	ACE2	4.26	82%
Toft et al.	222257_s_at	ACE2	5.18	57%
Toft et al.	1570433_at	TMPRSS2	3.30	0%
Toft et al.	205102_at	TMPRSS2	5.78	0%
Toft et al.	211689_s_at	TMPRSS2	3.34	0%
Toft et al.	226553_at	TMPRSS2	5.65	0%